Modelling of flow through potash tailings piles

D. K. H. WONG, S. L. BARBOUR, AND D. G. FREDLUND
Department of Civil Engineering, University of Saskatchewan, Saskatoon, Sask., Canada S7N 0W0

Received July 16, 1987
Accepted December 21, 1987

Modelling the flow of brine through potash tailings requires that the saturated and unsaturated hydraulic properties of the tailings be established; in particular, the relationships of fluid content and permeability to matric suction are required. The *in situ* and laboratory testing techniques used for determining these properties are described and the results are presented.

Numerical modelling techniques for the flow of brine through potash tailings are demonstrated by performing a computer simulation of an open-trench infiltration test conducted at the Lanigan Division Potash Mine in Saskatchewan. The responses of the field instrumentation during the infiltration test were compared with the results of the simulation. The simulation utilizes the measured fluid content versus suction curves and the calculated permeability versus suction curves as input parameters. Good agreement was observed between the measured and simulated field responses. The effects of varying the hydraulic properties of the tailings are examined to arrive at a better understanding of the flow mechanism involved.

Key words: saturated–unsaturated, seepage, finite element modelling, brine, potash, tailings, infiltration.

La mise au point d'un modèle pour l'écoulement de saumure à travers des résidus de potasse nécessite la détermination des propriétés hydrauliques saturées et non saturées des résidus; en particulier, les relations entre la teneur en fluide et la perméabilité par rapport à la matrice de succion sont requises. L'on décrit des techniques d'essais en laboratoire et *in situ* pour déterminer ces propriétés et présente les résultats des essais.

Des techniques de modèles numériques pour l'écoulement de la saumure à travers les résidus de potasse sont illustrées en réalisant une simulation à l'ordinateur d'un essai d'infiltration dans une tranchée ouverte réalisée à la Lanigan Division Potash Mine en Saskatchewan. Les réactions de l'instrumentation sur le chantier au cours de l'essai d'infiltration ont été comparées aux résultats de la simulation. La simulation utilise les courbes de teneur en fluide mesurée en fonction de succion et de perméabilité calculée en fonction de succion comme paramètres d'entrée. Une bonne concordance a été observée entre les réactions simulées et celles mesurées en place. L'influence de la variation des propriétés hydrauliques des résidus est étudiée de façon à en arriver à une meilleure compréhension du mécanisme d'écoulement empliqué.

Mots clés : saturé–non saturé, écoulement, modèle d'éléments finis, saumure, potasse, résidus, infiltration.

[Traduit par la revue]

Can. Geotech. J. **25**, 292–306 (1988)

Introduction

The mining of potash in Saskatchewan produces potash tailings as a waste material. The tailings are composed of approximately 90% sodium chloride, 7–8% potassium chloride, and a trace amount of insoluble material that is often referred to as clay slimes. The tailings are transported in a brine slurry to the tailings facility and then spigotted onto a tailings pile. The current maximum height of tailings piles in Saskatchewan is in the range of 50–60 m. Only the bottom 3–5 m of tailings is saturated. There are 10 tailings piles in Saskatchewan.

There are concerns regarding the environmental impact of the tailings piles on the existing groundwater, the operating brine balance within the piles, and the stability of the piles. To address these concerns, an understanding of the infiltration and saturated–unsaturated flow of brine within the tailings is required.

Techniques to analyze one-dimensional infiltration into an unsaturated soil were initially developed in the soil science area. An analytical solution of one-dimensional infiltration was originally developed by Philip (1957) for fairly restricted boundary conditions and soil properties. To handle more general conditions, numerical schemes were developed. Freeze (1969) provides a listing of papers containing finite difference solutions for one-dimensional infiltration problems.

In geotechnical engineering, analyses of seepage through saturated–unsaturated soil were originally developed by focusing only on the saturated soil zone. The phreatic surface was erroneously considered to be the uppermost flow line. The focus of both analytic and numerical solutions was on defining the location of the phreatic surface (Casagrande 1937; Taylor and Brown 1967; Neuman and Witherspoon 1971).

General numerical solutions of multidimensional saturated–unsaturated flow using finite difference or finite element techniques were eventually developed by Freeze (1971), Neuman (1973), Papagianakis and Fredlund (1984), Lam *et al.* (1987), and others. These solutions are distinguished by the fact that they consider the entire soil zone as a continuum. It is this more general approach to analyzing fluid movement through the unsaturated zone that will be used in this work.

For any of the above solution techniques, the basic physical relationships required for the analyses are fluid content versus matric suction and permeability versus matric suction. The latter relationship may be computed using the fluid content versus suction relationship and the coefficient of permeability of the saturated medium.

The *in situ* and laboratory testing techniques used to define the saturated and unsaturated hydraulic properites of the tailings have been presented by Wong and Barbour (1985, 1987); therefore, only a summary of the *in situ* and laboratory testing on the tailings is presented in this paper. The primary objective of this paper is to demonstrate the application of existing saturated–unsaturated flow theory and numerical modelling techniques to the analysis of flow of brine within a tailings pile.

Site description

The tailings facility selected for the study is located southeast of the Potash Corporation of Saskatchewan mine at Lanigan, which is situated about 100 km east of Saskatoon. Three study

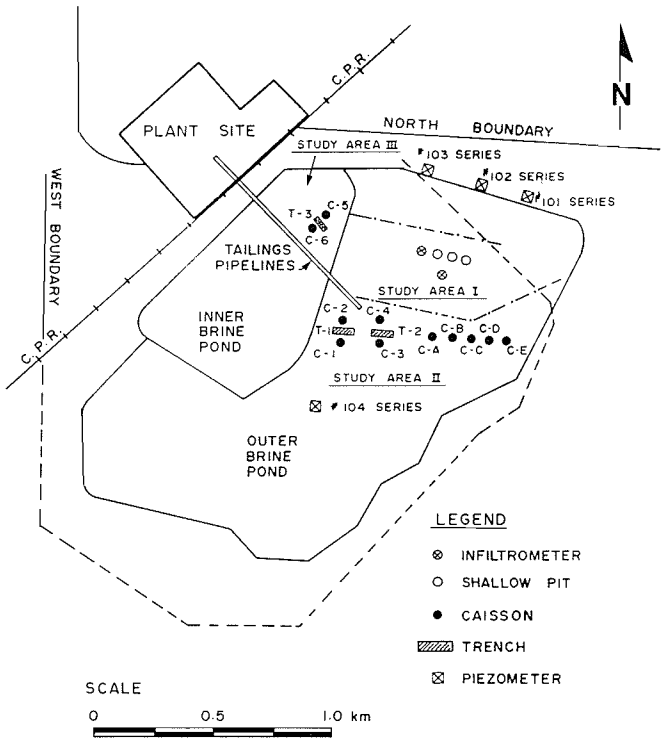

FIG. 1. Site plan.

areas within the tailings facility were chosen for the field program. The general layout of the test sites is shown in Fig. 1.

Since the beginning of operations in 1967, about 20×10^6 t of tailings have been deposited in the 270 ha tailings containment facility. The current height of the tailings pile is about 22 m. The tailings pile has been constructed by the conventional method of spigotting waste tailings that have been slurried with brine and pumped to the tailings facility. The tailings are deposited in cells bounded by low dykes constructed of tailings.

The tailings facility is located on a flat to gently undulating fluviolacustrine deposit consisting of sand, silt, and clay, which in turn is underlain by up to 180 m of glacial clay till.

Field test

Field testing consisted of a series of infiltration tests conducted on the tailings pile. The tests included single-ring infiltrometer, shallow-pit, open-caisson, and open-trench-type infiltration tests. The open-trench infiltration test was monitored for negative fluid pressures and fluid content within the tailings using tensiometers and neutron probes, respectively.

The results of the single-ring infiltrometer, shallow-pit, and open-caisson infiltration tests were used to assess the saturated permeability of the tailings. During these tests small amounts of air may still remain within the voids of the tailings; consequently, the term "field-saturated" will be used to distinguish the values of saturated permeability obtained by field testing from those obtained by laboratory testing on fully saturated samples.

Field-saturated permeability

Single-ring and shallow-pit infiltration tests were performed on the surface of the tailings pile at study area I. The use of a double ring is usually preferred in infiltration tests; however, the coarse and highly cemented nature of the potash tailings made it difficult to install and seal rings into the surface. The procedures for conducting the ring and pit infiltration tests were essentially the same. The single-ring infiltrometer tests consisted of setting metal rings into the surface of the tailings, whereas the shallow-pit infiltration tests required forming hand-dug shallow pits. In these two types of tests, constant levels of brine were maintained within the rings or shallow pits by adding brine obtained from a spigot discharge located nearby. Readings of the volume of brine added at successive time intervals were taken until a final steady infiltration rate was established. Depending on the pond height to radius ratio, the steady state condition was generally achieved within 45 min.

TABLE 1. Summary of field-saturated permeability

Test number	Test method	Calculated field-saturated coefficient of permeability (m/s)
1	Infiltrometer No. 1	1.59×10^{-5}
2	Infiltrometer No. 2	1.55×10^{-5}
3	Shallow pit No. 1	1.62×10^{-5}
4	Shallow pit No. 2	2.79×10^{-5}
5	Shallow pit No. 3	1.44×10^{-5}
6	Caisson A	3.99×10^{-5}
7	Caisson C	3.39×10^{-5}
8	Caisson D	3.65×10^{-5}

The field-saturated permeability is computed from the test results utilizing Darcy's law, and assuming that a unit vertical hydraulic gradient is approached when the infiltration rate is constant. The single ring and shallow pits used for these tests have a small pond height relative to the radius, and most of the flow will move vertically through the base of the ring or pit. Consequently, the field-saturated permeability calculated from these tests reflects predominantly the vertical permeability of the tailings (Kessler and Oosterbaan 1974).

The open-caisson infiltration test was conducted on the tailings pile at study area II. This test is essentially a scaled-up shallow-pit test in which the test is extended to greater depths. As a result, the lateral component of flow becomes a major component of brine infiltration. The test was conducted in a manner similar to that described for the single-ring and shallow-pit infiltration tests.

The method presented by Reynolds *et al.* (1983), which accounts for the predominantly lateral flow component developed in this test, was used to assess the field-saturated permeability. The method takes into account pressure- and gravitation-induced fluxes along the wall and base of the caisson. The field-saturated permeability obtained from this test is dominated by the horizontal permeability of the tailings due to the relatively large height-to-radius ratio of the caisson.

The field-saturated coefficients of permeability for the single-ring, shallow-pit, and open-caisson infiltration tests are summarized in Table 1. The different test methods appear to give consistent results. The permeabilities calculated from the open-caisson infiltration tests are approximately a factor of 2 larger than those from the single-ring and shallow-pit infiltration tests. This would suggest that a significant degree of anisotropy is present within the tailings.

Field fluid content versus suction curve

The fluid content versus suction curve was established by monitoring fluid pressures and fluid contents within the tail-

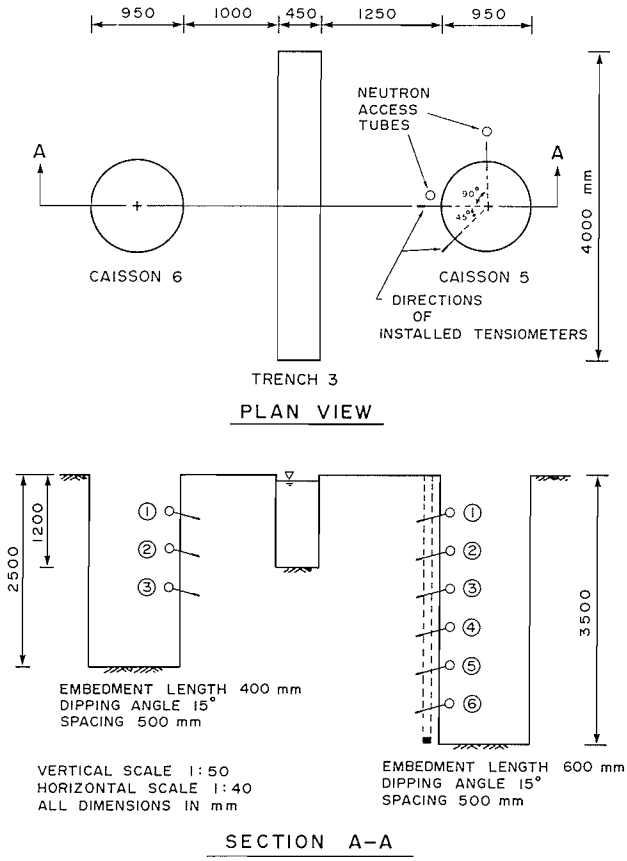

FIG. 2. Layout of the trench infiltration test at study area III.

ings, using tensiometers and neutron probes installed at the open-trench infiltration site at study area III. The general layout of the test trench, caissons, and instrumention is illustrated in Fig. 2.

The test was conducted after a series of initial readings had been obtained from the tensiometer and neutron probes. Brine was transported to the site from the brine pond using two 5000 l water tanks. Brine was added to the trench, and a constant brine level 1.0 m above the base of the trench was maintained until the available brine was depleted, after which time the trench was allowed to drain. The flow rate required to maintain the brine level was monitored using a flowmeter. Tensiometer readings and 1 min counts from the neutron probes were made at regular intervals throughout the test. Additional tensiometer and neutron probe readings were obtained 24 h after the test was conducted.

Typical sets of corresponding tensiometer and neutron probe responses during the open-trench infiltration test are plotted in Figs. 3*a*–3*d*. In general, the form of the tensiometer response diagrams are "mirror images" of the neutron probe response diagrams. As the brine front passes, rapid decreases in suction from the tensiometer readings correspond with sharp increases in volumetric fluid content from the neutron probe readings. Similarly, as the tailings drain after infiltration is stopped, slow increases in suction correspond with slow decreases in volumetric fluid content. At a depth of 2 m, it can be seen that no abrupt change in the suction and volumetric fluid content occurs with the advance of the brine front. In addition, the initial suction values were maintained constant for a much longer time at these locations than at the locations situated above. The reason for these phenomena is the presence of a slime layer, approximately 50 mm thick, located at about 2 m from the tailings surface. Owing to its low permeability, this slime layer impeded the infiltration process. As a consequence, the potash tailings located beneath the slime layer experience lower rates of infiltration.

Laboratory tests

In the laboratory, tests were conducted to determine the index properties of the tailings and the fluid content versus suction curves for both the tailings and clay slimes. All tests were performed using potash tailings brine as a pore fluid.

Index properties

The index properties of the tailings, such as gravimetric fluid content, bulk density, and dry density, were studied. The gravimetric fluid content is defined as the ratio of the mass of brine solution to the mass of solid particles. Evaluation of the bulk density and gravimetric fluid content of the tailings was conducted on block samples obtained from the trench test site. Dry density was calculated from the corresponding set of values of bulk density and gravimetric fluid content. The bulk density was found to increase slightly with depth, with values ranging from 1.37 Mg/m^3 at the surface to 1.64 Mg/m^3 at a depth of 3 m. The gravimetric fluid content varied from 2 to 5% in the same depth range.

Laboratory fluid content versus suction curve

The fluid content versus suction curves of the tailings and the clay slimes were determined in the laboratory using a commercially available apparatus called the Tempe pressure cell.[1] The Tempe pressure cell operates under the same physical principles as the porous-plate apparatus described in ASTM D 2325-68 and ASTM D 3152-72.

Duplicate undisturbed tailings core samples at various depths ranging from the tailings pile surface to a depth of 3.0 m were used in this investigation. Undisturbed core samples were prepared on a lathe using block samples obtained from the test site. Measurements were made on only three disturbed clay slimes core samples, owing to the difficulty in obtaining an undisturbed core sample from the slime layer inside the test caissons.

The results of the Tempe pressure cell tests on the tailings and clay slimes are plotted as suction against volumetric fluid content in Figs. 4*a* and 5*a* respectively. Using the fluid content versus suction curve and an estimate of the saturated coefficient of permeability, the permeability versus suction relationship can be calculated using the method described by Green and Corey (1971) and Elzeftawy and Mansell (1975). The calculated relationship between permeability and suction is shown in Figs. 4*b* and 5*b* for the tailings and clay slimes.

Computer modelling

A numerical simulation of infiltration of brine through the tailings during the trench infiltration test was performed using a transient saturated–unsaturated finite element flow model. The computer flow model, TRASEE, was developed at the University of Saskatchewan (Lam 1983; Lam *et al.* 1987). The purpose of this simulation was to verify the application of the simulation model to the flow of brine in the tailings, and to

[1]Soil Moisture Equipment Corporation, P.O. Box 30025, Santa Barbara, CA 93105, U.S.A.

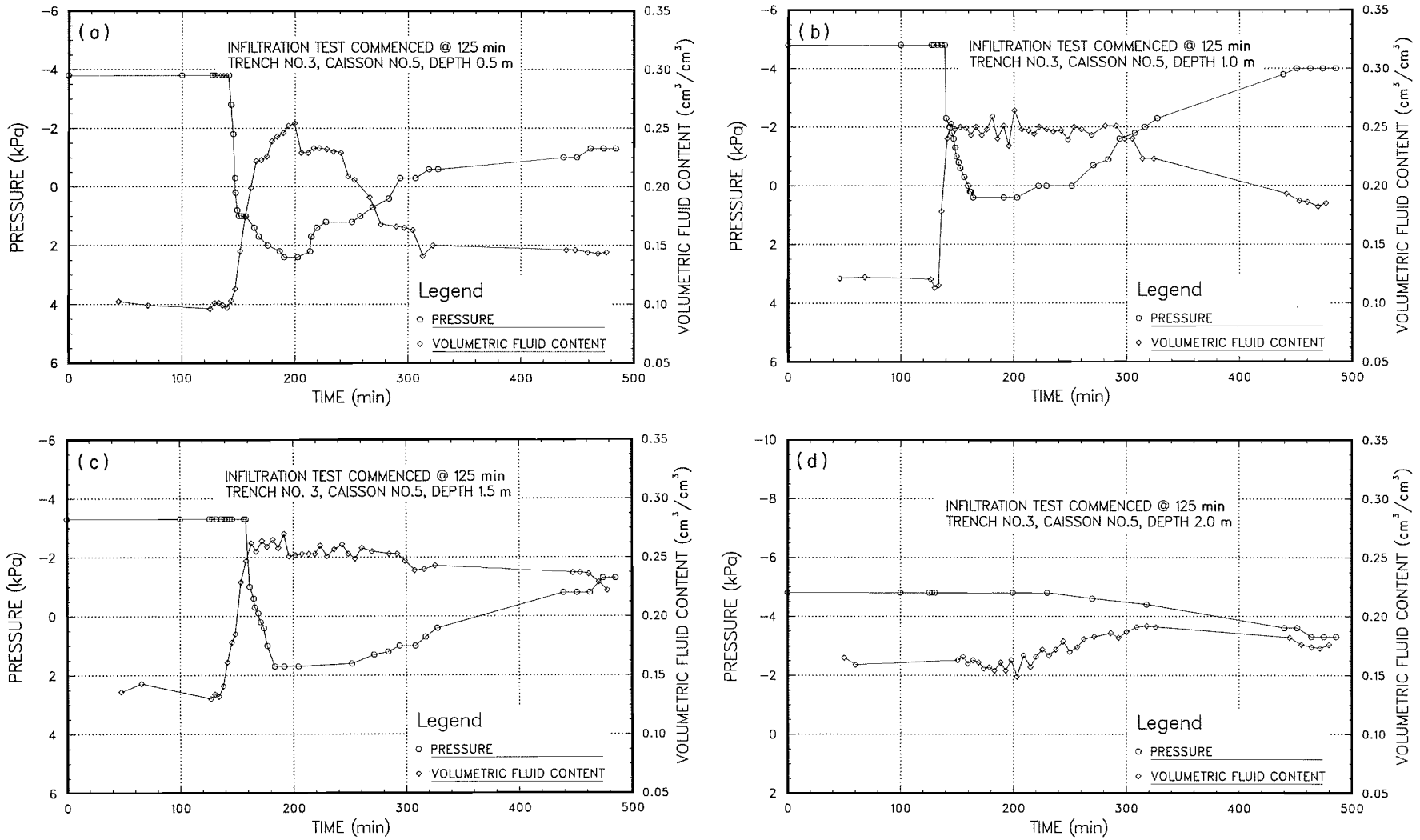

FIG. 3. Responses of tensiometer and neutron probe at (*a*) 0.5 m, (*b*) 1.0 m, (*c*) 1.5 m, and (*d*) 2.0 m.

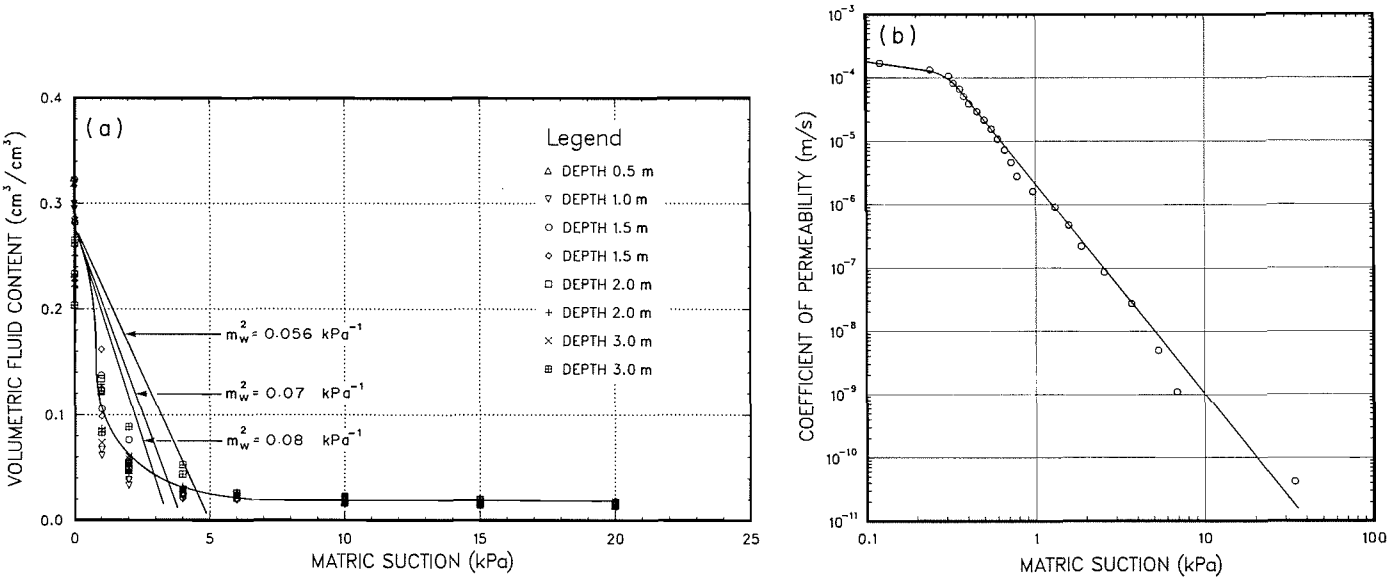

FIG. 4. (*a*) Laboratory fluid content – suction curve for potash tailings; (*b*) calculated permeability–suction relationship for potash tailings.

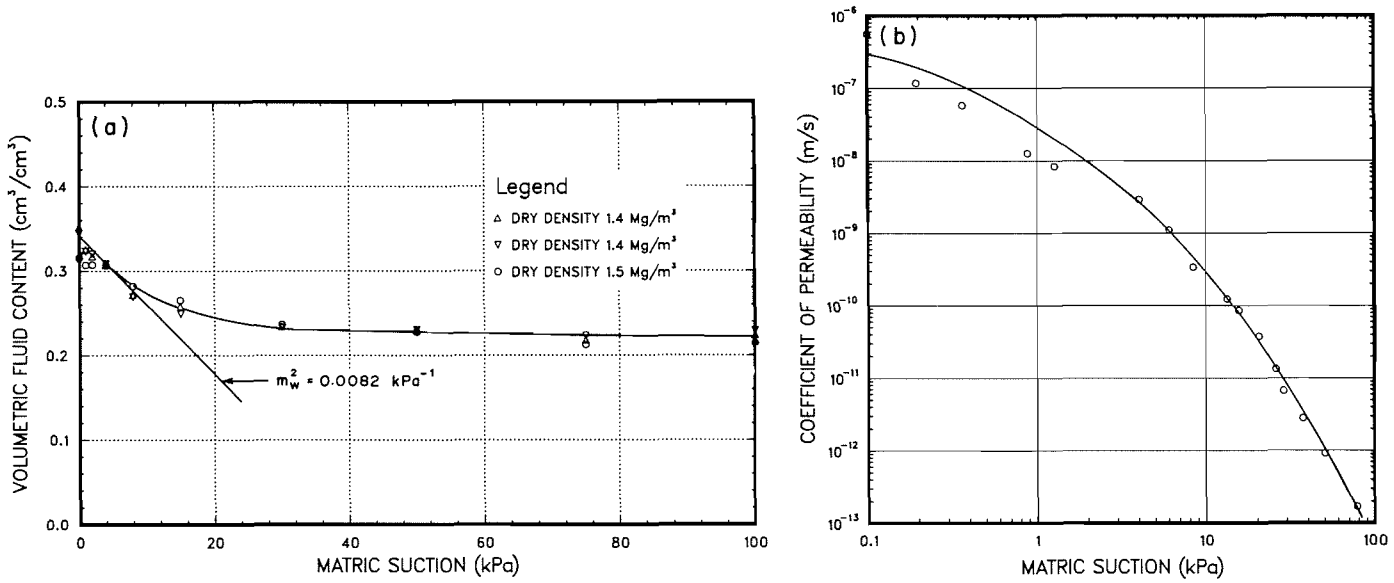

FIG. 5. (*a*) Laboratory fluid content – suction curve for clay slimes; (*b*) calculated permeability–suction relationship for clay slimes.

examine the application of the measured fluid content versus suction curves and calculated permeability functions.

Finite element flow model

The general description of the flow model and its theory are described in the following sections.

General description

The model describes fluid flow in a two-dimensional saturated–unsaturated soil system by applying Darcy's law to both zones. In the saturated zone, the coefficient of permeability is regarded as a constant. In the unsaturated zone, however, it is considered to be a function of negative fluid pressures. Changing fluid contents with suction are incorporated into the model utilizing a storage term, m_2^w, which is the slope of the fluid content versus suction curve. The soil skeleton is assumed to be nonswelling, and the fluid phase is assumed to be incompressible.

It is assumed that the air phase within the unsaturated zone is continuous and under atmospheric pressure. Therefore, the model considers only the flow of the liquid phase. The assumption that the flow of air is unrestricted is reasonable considering the low initial fluid content and the coarse texture of the tailings.

The model formulation is based on the Galerkin technique of the weighted-residual method. A time-centred, Crank–Nicholson, or backward finite difference scheme is employed to march forward with time in the transient flow process.

Theory

Darcy's law can be used to express the net flux of fluid per unit volume of an element under isothermal conditions:

$$[1]\quad \frac{\partial \theta_w}{\partial t} = -\left[\frac{\partial}{\partial x}\left(k_x \frac{\partial h}{\partial x}\right) + \frac{\partial}{\partial y}\left(k_y \frac{\partial h}{\partial y}\right)\right]$$

where θ_w = volumetric fluid content of the element; k_x, k_y = coefficient of permeability with respect to the x, y directions, respectively; and h = hydraulic head (i.e., $h = u_w/\rho_f g + y$).

Fredlund and Morgenstern (1976) proposed a constitutive relationship linking the stress and deformation state variable. Their constitutive relationship for the fluid phase of an unsaturated medium is

$$[2] \quad \theta_w = m_1^w \, d(\sigma - u_a) + m_2^w \, d(u_a - u_w)$$

where m_1^w = slope of the $(\sigma - u_a)$ versus θ_w plot when $d(u_a - u_w)$ is zero; m_2^w = slope of the $(u_a - u_w)$ versus θ_w plot when $d(\sigma - u_a)$ is zero; σ = total stress; u_a = pore-air pressure; and u_w = pore-fluid pressure.

This constitutive equation for the liquid phase can be differentiated with respect to time and substituted into [1]. If it is assumed that the m_1^w, m_2^w, and σ variables are constant during the transient process, the resulting equation can be written as follows:

$$[3] \quad \frac{\partial}{\partial x}\left(k_x \frac{\partial h}{\partial x}\right) + \frac{\partial}{\partial y}\left(k_y \frac{\partial h}{\partial y}\right) = \rho_f g m_2^w \frac{\partial h}{\partial t}$$

A more general governing equation, where the major coefficient of permeability is at an angle to the x-axis, can be expressed as follows (Lam *et al.* 1987):

$$[4] \quad \frac{\partial}{\partial x}\left(k_{xx} \frac{\partial h}{\partial x} + k_{xy} \frac{\partial h}{\partial y}\right) + \frac{\partial}{\partial y}\left(k_{yx} \frac{\partial h}{\partial x} + k_{yy} \frac{\partial h}{\partial y}\right) = \rho_f g m_2^w \frac{\partial h}{\partial t}$$

where k_{xx}, k_{xy}, k_{yx}, k_{yy} = permeability tensor of an anisotropic medium.

Simulation input parameters

Two basic concerns in the numerical simulation of transient flow are the selection of appropriate physical properties and the selection of appropriate model characteristics, such as grid size, time step, and initial boundary conditions.

Functional relationship between suction, fluid content, and permeability

Earlier works performed by Wong and Barbour (1985, 1987) have shown that good agreement was obtained between the fluid content versus suction curves determined from the field and those obtained from laboratory testing.

The fluid content versus suction curves obtained by the Tempe pressure cell tests are based upon the static equilibrium technique. It is common practice to use these relationships in the analyses of both steady-state and transient unsaturated flow problems (Elzeftawy and Mansell 1975). The assumption made in these analyses is that the fluid content versus suction curve is independent of the state of flow. The uniqueness of the fluid content versus suction curve has been studied by a number of investigators, However, the published test results in the literature are somewhat contradictory (Watson 1965; Smiles *et al.* 1971; Vachaud *et al.* 1972).

In general, the test results appeared to indicate that the discrepancy between the static and transient curves occurs only at intermediate suction values, good agreement being obtained at low and high suction values. In addition, it is noted that the larger the saturated coefficient of permeability and the smaller the suction gradient, the smaller will be the divergence between transient and static relationships (Vachaud *et al.* 1972).

In view of the fact that the tailings exhibit comparatively high saturated permeability and low suction values in the field, it is assumed that the discrepancy between the transient and static relationships would be insignificant. In the case of the clay slime material, the geometric uncertainties involved in the assumption that the slime layer occurred in the field as a uniform and homogeneous stratum, and in the utilization of only a few samples to characterize the entire slime layer will overshadow secondary influences of the flow-dependent properties of the material.

In light of the foregoing discussion, the fluid content versus suction curves for both the tailings and clay slimes determined from the Tempe pressure cell tests were used in all simulations. The actual fluid content versus suction curves were approximated using different storage terms, m_2^w, calculated from the average slope of the curves over the pressure range of concern, as shown in Figs. 4*a* and 5*a* for the tailings and the clay slimes, respectively. This numerical technique, called linearization, has been successfully utilized by Segol (1982) to alleviate the numerical difficulties commonly encountered in solving the nonlinear equation at a scale appropriate to field problems.

Two different simulations, designated A and B, were conducted in this study. To better approximate the actual fluid content versus suction curve for the tailings, three different values of m_2^w depending on the initial suction values were selected, along with m_2^w of 0.0082 kPa^{-1} for the clay slimes in simulations A and B (Figs. 4*a* and 5*b*). In addition, various values of m_2^w equal to 1/5 of the corresponding m_2^w assigned to the negative pore-fluid pressure zone were incorporated in the positive pore-fluid pressure zone in simulation A. In simulation B, the same constant average values of m_2^w used in the negative pore-fluid pressure zone were also utilized in the positive pore-fluid pressure zone.

In addition, the permeability functions calculated from the fluid content versus suction curves determined in the laboratory were used. Representative saturated coefficients of permeability for the tailings and clay slimes as obtained by laboratory testing were used because no specific infiltration tests for evaluating saturated permeability were undertaken in study area III. All the relevant parameters used in simulations A and B are summarized in Table 2.

Heterogeneity and anisotropy

In unsaturated porous media, it is important to distinguish the difference between heterogeneity and anisotropy on the basis of scale. McWhorter (1985) suggested that macroscopic stratification of several centimetres' thickness within a formation should be considered as heterogeneous and be treated by analyzing the flow in the individual strata with appropriate hydraulic properties. On the other hand, microscopic stratification should be regarded as anisotropic and be analyzed by assigning directional properties to the coefficients of permeability.

Heterogeneity was encountered in the test site at study area III because of the presence of a distinct slime layer embedded within the tailings formation. This heterogeneity was taken into account by assigning appropriate hydraulic parameters to each individual material.

A significant degree of anisotropy was present within the tailings, as suggested by the difference between the calculated horizontal and vertical permeabilities determined by the various infiltration tests in study areas I and II. In the absence of

Table 2. Summary of parameters used for modelling

Material	Simulation	m_2^w (kPa^{-1}) Negative pressure zone	m_2^w (kPa^{-1}) Positive pressure zone	k_h/k_v	k_h ($\times 10^{-4}$ m/s)	k_v ($\times 10^{-4}$ m/s)	Permeability–suction relationship
Potash tailings	A	f (initial suction) value	1/5 of the corresponding storage term in negative pressure zone	5.0	2.21	0.44	Based on laboratory fluid content – suction curve
	B	f (initial suction) value	Same storage terms as in the negative pressure zone	5.0	2.21	0.44	Based on laboratory fluid content – suction curve
Clay slimes	A	Constant (0.0082)	1/5 of the corresponding storage term in negative pressure zone	1.0	0.0055	0.0055	Based on laboratory fluid content – suction curve
	B	Constant (0.0082)	Same storage term as in the negative pressure zone	1.0	0.0055	0.0055	Based on laboratory fluid content – suction curve

NOTE: m_2^w = storage term; k_h = coefficient of permeability in horizontal direction; k_v = coefficient of permeability in vertical direction.

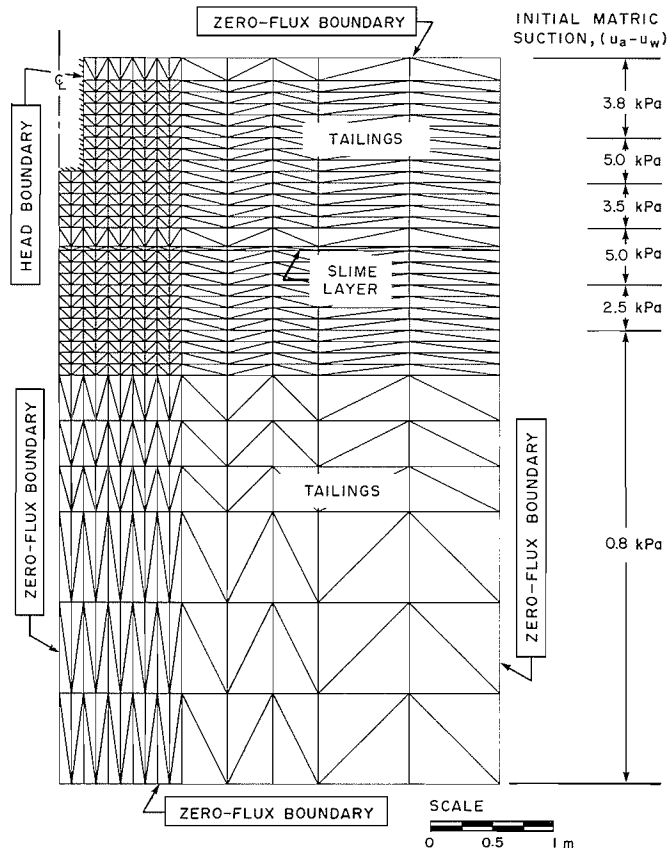

FIG. 6. Finite element mesh, and boundary and initial conditions used in the simulation.

field data regarding the ratio of horizontal to vertical permeability in study area III, a value of 5 was used to represent the degree of anisotropy of the tailings at this location. This value was based on a series of trial-and-error analyses conducted in simulations A and B.

Grid size and time step

Appropriate choices of grid size and time step are of considerable practical importance in solving a given problem efficiently and economically. In addition, the right combination of spatial and time discretization not only gives solutions with acceptable accuracy but also minimizes the occurrence of instability in the simulation.

Figure 6 shows the finite element mesh used in the simulation models. By taking advantage of an axis of symmetry, only half of the test section was required for analysis. The size of the finite element mesh was chosen sufficiently large so that influence of a zero-flux boundary at the top, bottom, and right-hand boundaries of the model would be negligible. In general, fine grids were used where instrumentation was installed and details of changes in pressure heads were of importance. On the other hand, coarse grids were used where details were of secondary interest. In selecting the grid spacing, it was felt that an adequate degree of discretization would be provided if, under an arbitrary hydrostatic condition, the fluid content versus suction could be intercepted several times within the full range of fluid contents by the vertical grid spacing. This resulted in a finest vertical grid spacing of 12.5 cm being chosen for the simulations. In a similar manner, small time steps were chosen where rapid changes in pressure heads were

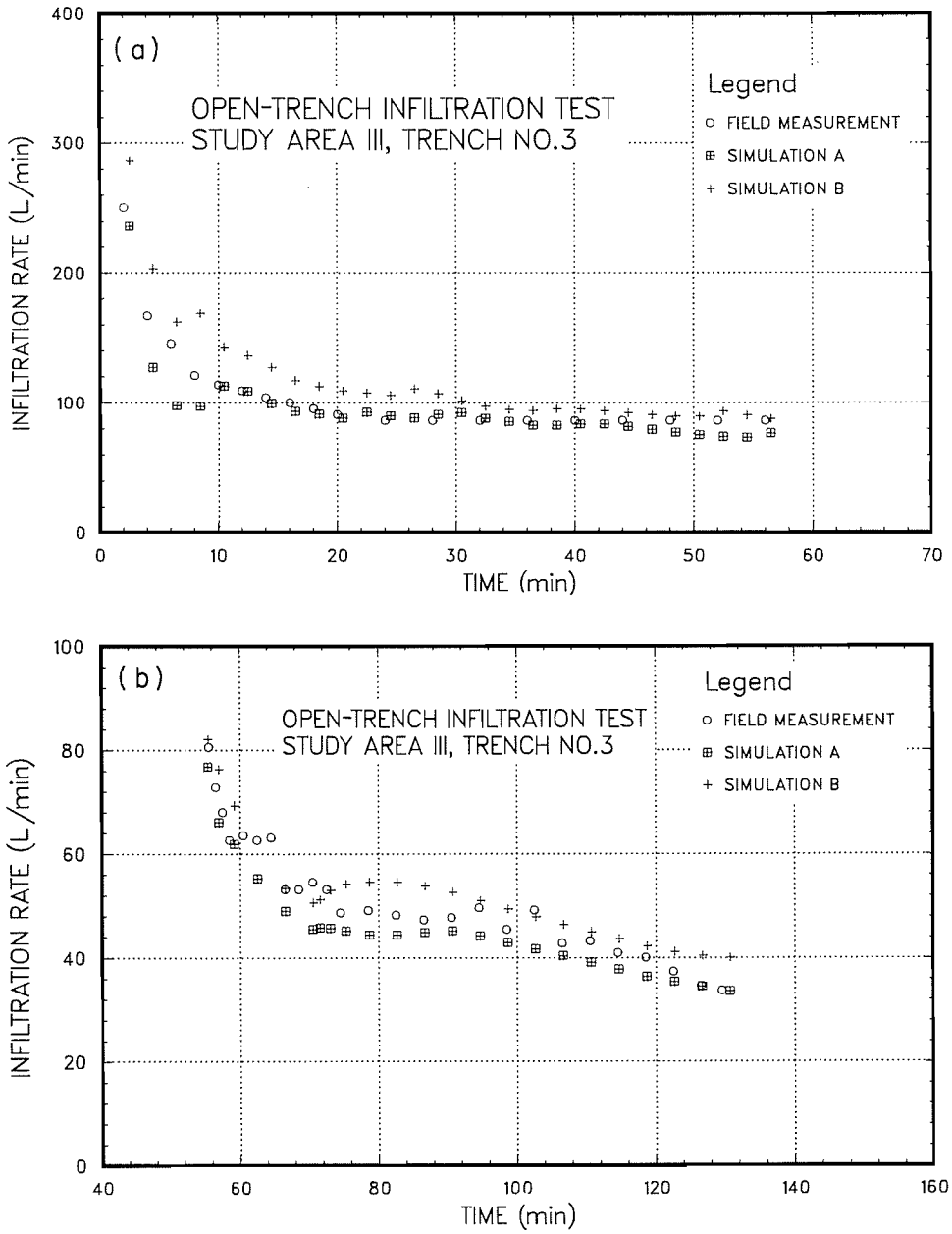

FIG. 7. Comparison of field-measured and computer-simulated infiltration rate curves: (*a*) for the initial 55 min; (*b*) after the initial 55 min.

anticipated during the transient infiltration process. On the other hand, progressively larger time steps were adopted where changes in pressure heads were much more gradual, such as occurred during the transient drainage process.

Initial and boundary conditions

Additional information regarding the initial and boundary conditions is required in order to simulate the transient flow process corresponding to the infiltration test in the field. The initial conditions are the values of the dependent variable specified within the boundary, whereas the boundary conditions are the values of the dependent variable at the boundary or its spatial derivative normal to the boundary. For unsaturated flow problems, this consists of specifying the hydraulic head at the boundary or the seepage flux across the boundary.

The appropriate initial and boundary conditions for simulations A and B are shown in Fig. 6. Measured tensiometer readings prior to the infiltration test were used as initial conditions in simulations A and B. Values in the form of hydraulic head were specified at every node within the defined boundary. In addition, zero-flux boundary conditions were specified at all the boundaries except at the trench. Along this boundary, both a constant-head boundary and a changing-head boundary were applied. The changing-head boundary conditions were specified along the boundary at the trench in accordance with the rate of change of brine level inside the trench. All the head boundary conditions were specified in the form of hydraulic heads.

Results and discussions

Comparisons of field-measured and computer-simulated results

Comparisons of the field-measured infiltration rates with that predicted by simulations A and B are illustrated in Figs. 7*a* and

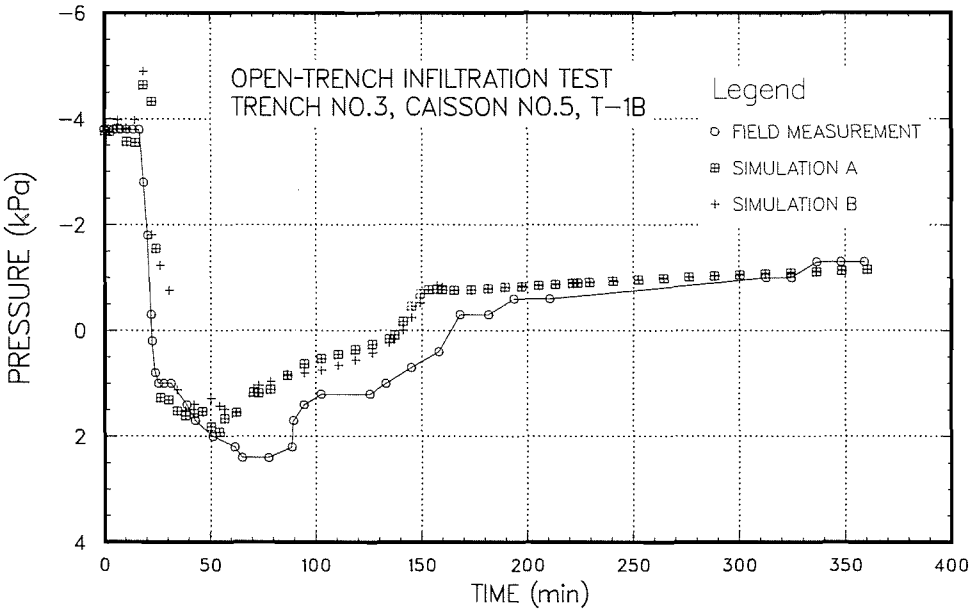

FIG. 8. Comparison of field-measured and computer-simulated pressure response (tensiometer No. T-1B).

7*b* respectively. Figure 7*a* shows the comparison of the infiltration rate for the initial 55 min during the trench infiltration test, whereas Fig. 7*b* indicates the comparison after the initial 55 min. The results show good agreement between the field-measured and -simulated infiltration rates, especially at the final steady state. This indicates a good approximation of the saturated coefficient of permeability determined from the laboratory testing as well as of the degree of anisotropy. The initial portion of the infiltration curve shows some discrepancies that are related to the estimate of the permeability function and storage term.

The effect of adopting different storage terms in the region of positive and negative pore pressures in simulation A and a constant storage term in simulation B is demonstrated in Figs. 7*a* and 7*b*. In general, simulation B shows a slightly higher infiltration rate at any given time when compared with simulation A. The reason for the slightly higher infiltration rate is the fact that by extending the storage term linearly into the positive pressure zone increased storage of brine occurs, with the development of positive pressure within the tailings. Simulation A is likely more theoretically correct than simulation B, since it describes a distinct change in storage term in the relationship between volumetric fluid content and pressure when the pressure goes from negative to positive.

For an incompressible medium, the storage term relating volumetric fluid content and pressure at saturation in the positive pressure range is equal to zero. It was observed in the numerical analyses that utilizing zero values of m_2^w in the positive pressure range or values of m_2^w of 1/5 of the corresponding m_2^w in the negative pressure range does not produce any significant differences in the simulated results, in terms of infiltration rates or pressure responses. The use of a zero value of m_2^w in the positive pressure range produces an unacceptable degree of numerical instability. The numerical instability is caused by the transition between the relatively flat slope in the positive pressure range and the relatively steep slope in the negative pressure range.

As shown in Fig. 7*a*, the predicted infiltration curve from simulation A agrees better with the field curve than that from simulation B, especially for the initial 55 min. After the initial 55 min, the predicted infiltration rates from simulation A are slightly lower than the field measurements and are likely due to interference of the caisson in the field. In addition, it is also noted that the presence of the slime layer in the field greatly reduces the infiltration rate at the 55 min mark. This is illustrated in both the field measurements and the simulated results as shown in Fig. 7*b*.

The agreement between the simulated pressure responses of the tensiometers and those monitored in the field was variable. Good agreement between the measured and simulated responses appeared to be dependent on the spatial locations of the tensiometer tips with respect to the locations of the caisson, as well as the slime layer. The modelling work was complicated to a certain extent by the presence of the slime layer located at about 2 m from the tailings surface as well as the caissons situated on either side of the test trench. To obtain a realistic simulation, the presence of this distinct slime layer must be incorporated in the simulation models. However, characterization of the clay slimes appeared to be a problem owing to the difficulty in obtaining undisturbed samples from the slime layer for laboratory testing. In addition, the presence of the caisson also gave rise to a dimensional incompatibility problem, since a long narrow trench could be idealized as a two-dimensional problem but a caisson could not. It should be realized, however, that the dimensional problem would have become less significant had there been no slime layer present.

Figures 8 and 9 indicate that the predicted pressure responses from simulations A and B show good agreement with the field measurements. The apparent difference in pressure values between the initial portions of the predicted and measured pressure response curves, as shown in Fig. 9, occurs because suction readings as measured by the B-series tensiometers were used as initial conditions in the simulation models instead of the readings from the A-series tensiometers. The B-series tensiometers were installed normal to the longitudinal axis of the trench, whereas the A-series tensiometers were installed at an angle of 90° measured horizontally from the trench side of the caisson (Fig. 2).

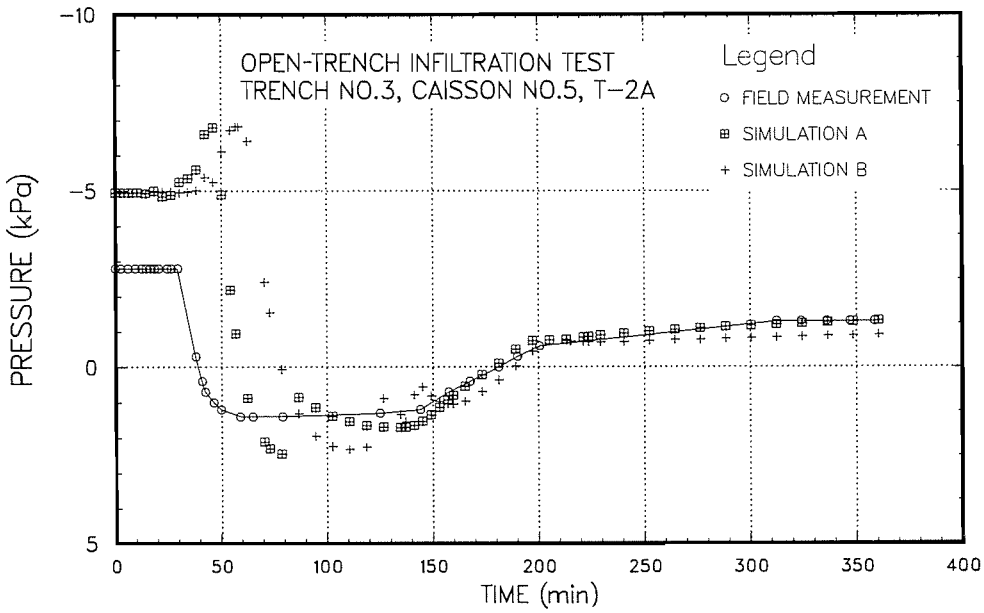

FIG. 9. Comparison of field-measured and computer-simulated pressure response (tensiometer No. T-2A).

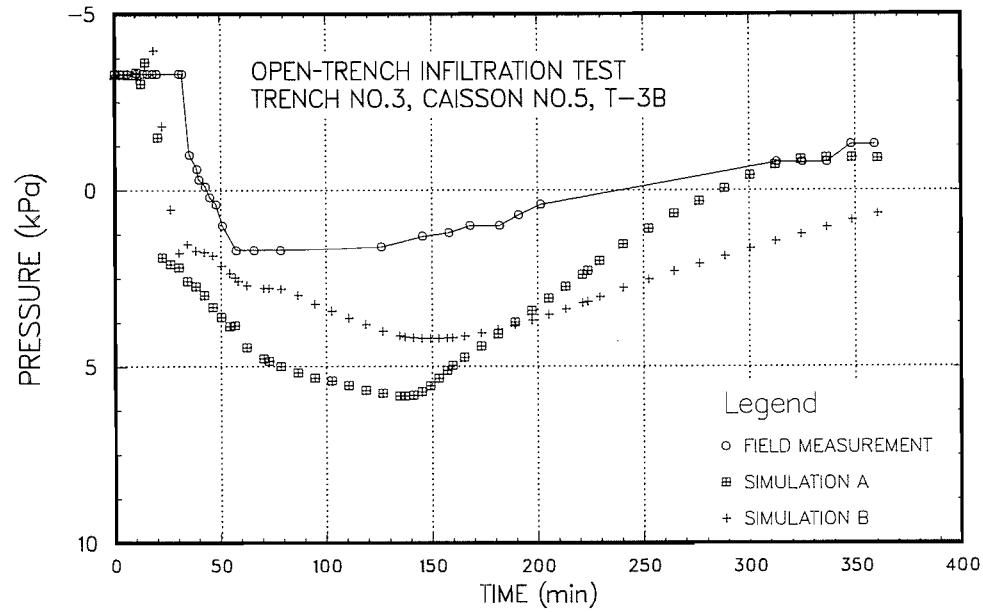

FIG. 10. Comparison of field-measured and computer-simulated pressure response (tensiometer No. T-3B).

Earlier numerical simulations described by Wong and Barbour (1985) have illustrated that the numerical oscillations of the pressure values near the time at which the wetting front passes the tensiometer tips were related to the time and space discretizations used in the simulation models. Although the problem of numerical instability as shown in Fig. 8 and 9 has largely been resolved through a refinement of the temporal and spatial discretization, it is considered that a complete elimination of the observed numerical instability is difficult. This is because of a material with a strongly nonlinear permeability property is being dealt with in this study.

A good estimate of the storage term is required to obtain an accurate prediction of the arrival time of the wetting front. As shown in Fig. 8, the predicted arrival time of the wetting front is in agreement with the field measurements, indicating a good estimate of the storage term. On the other hand, the arrival time of the wetting front predicted by simulation B shows a slower response compared with that of the field measurements, as indicated in Fig. 9. However, the matching of the arrival time of the wetting front was improved by adopting a smaller storage term as illustrated by the predicted result obtained from simulation A in Fig. 9.

Figures 10 and 11 present the pressure responses for the locations at which the influence of the caisson becomes more predominant. All the simulated pressure response curves shown in these figures have trends similar to the measured ones, despite the influence of the caisson. In general, the results appear to indicate that discrepancies between the simulated and field-measured pressure response curves only occur at some intermediate stage during the trench infiltration test

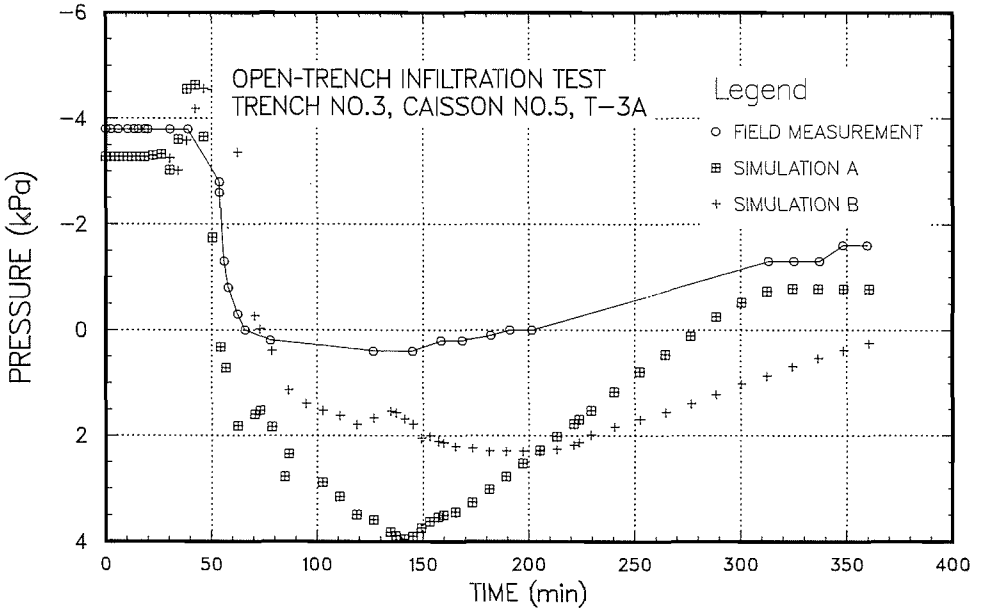

FIG. 11. Comparison of field-measured and computer-simulated pressure response (tensiometer No. T-3A).

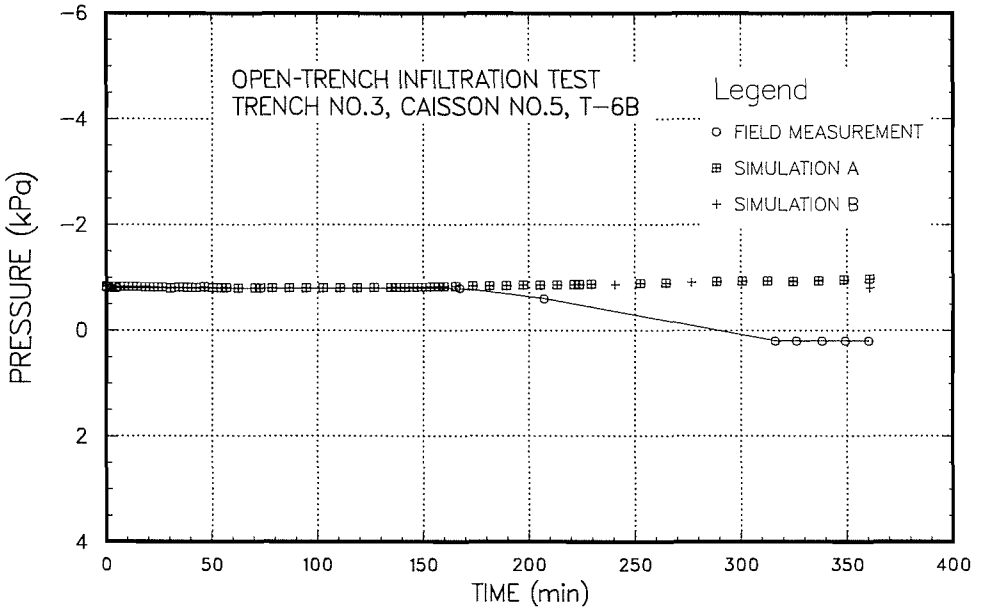

FIG. 12. Comparison of field-measured and computer-simulated pressure response (tensiometer No. T-6B).

and reasonable agreements are obtained at the initial and final stages of the test. The discrepancies are attributed to the presence of the caisson in the field, which imposed a rapid change in the boundary condition, causing pressure relief at the edge of the caisson during the intermediate stages of the test. Field observations verified that a seepage face developed at the caisson, during the test. This provides an explanation of why the field pressure response curves indicate smaller positive pressure values compared with the simulated ones.

The effect of utilizing different storage terms in simulation A and a constant storage time in simulation B is further illustrated by the plots shown in Figs. 10 and 11, respectively. In general, all the pressure response curves predicted by simulation A appeared to reach higher positive pressures, and recovered from these positive pressures at a faster rate than those predicted by simulation B. The reason for this is that a much smaller storage term is employed in simulation A, which, in effect, would cause a large change in pressure with a small change in volumetric fluid content.

Only marginal agreement was obtained between the measured and simulated response curves for the locations underneath the slime layer. This is attributed to the previously mentioned difficulty in characterizing the slime layer, as well as the abrupt changes in permeability at the interface between the tailings and the slime layer. A typical plot pertaining to the comparisons of the field-measured and computer-simulated pressure responses at these locations is shown in Fig. 12.

Sensitivity analyses of the input parameters

Sensitivity analyses of the input parameters were carried out

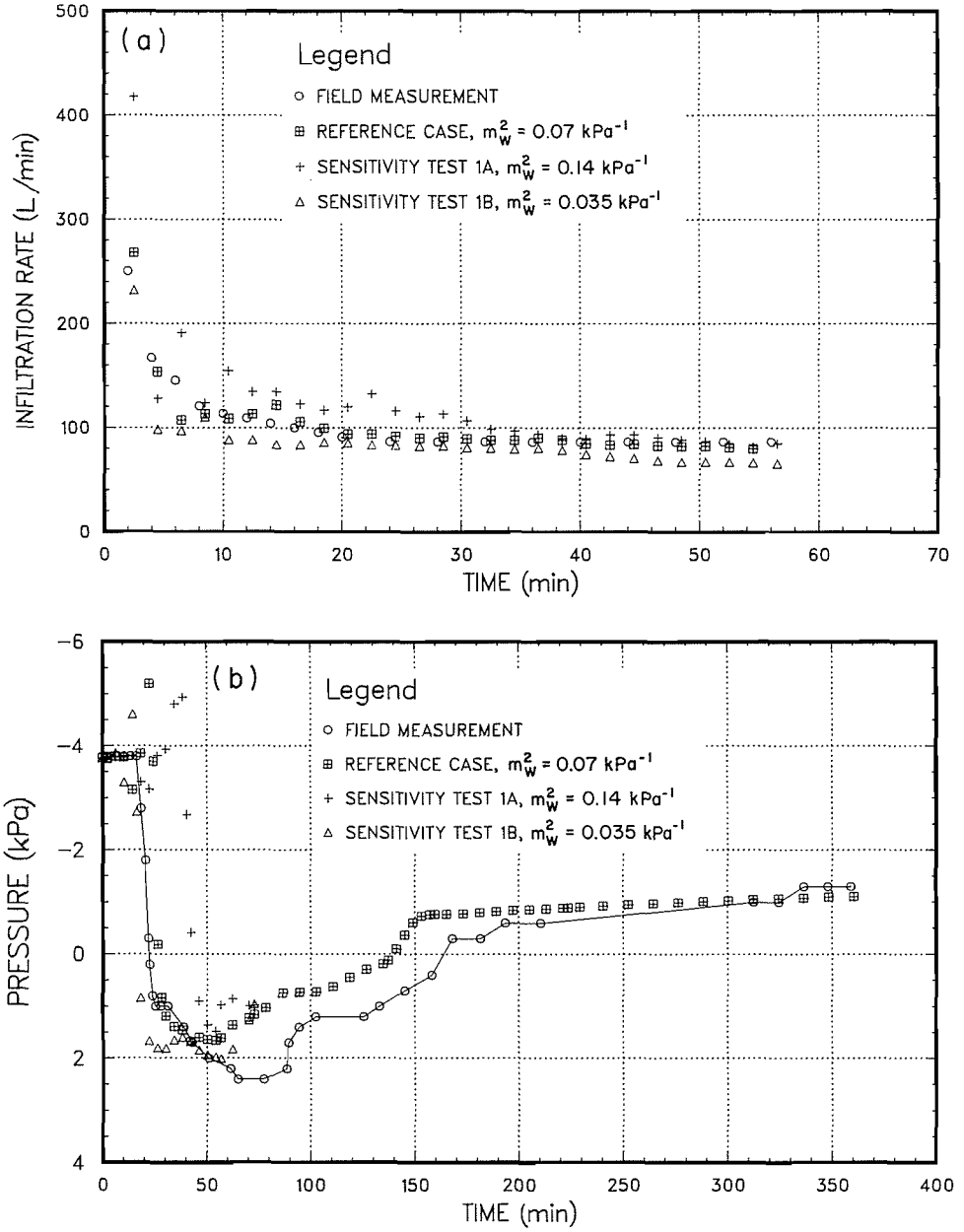

FIG. 13. (*a*) Effect on infiltration rate due to variation of storage term; (*b*) effect on pressure response due to variation of storage term.

in an attempt to examine the resulting impacts on the simulated results, in terms of both infiltration rate and pressure response. In particular, three different sensitivity tests were preformed by varying the storage term and the vertical and horizontal coefficients of permeability. A reference case was employed to facilitate the comparisons. This has the same input parameters as simulation A except that a constant storage value for the tailings was used. In each of the sensitivity tests, only one specific input parameter was allowed to increase and decrease, by a factor of 2, with respect to the input parameter of the reference case so that the influence of that particular input parameter could be examined.

Figures 13*a* and 13*b* illustrate the effects of the storage term on the simulated infiltration rates and pressure responses respectively. As shown in Fig. 13*a*, the storage term affects the initial infiltration rates to a certain extent but does not produce any significant effects on the final steady state infiltration rates. However, it does produce marked influences on the arrival time of the wetting front, as demonstrated by the simulated pressure response curves in Fig. 13*b*. A larger storage term would cause a delayed arrival of the wetting front, whereas a smaller one would hasten its arrival. In addition, it was also observed that a larger storage term caused more iterations in the computation as well as more numerical instabilities.

The influences of the vertical coefficients of permeability on the simulated infiltration rates and pressure responses are shown in Figs. 14*a* and 14*b* respectively. Figure 14*a* shows that the vertical permeability has little to no influence in the initial stages of the infiltration rates but it has a more definite effect on infiltration rates at final steady state. It does not, however, have any significant influences on the pressure response with respect to the arrival time of the wetting front (Fig. 14*b*). In general, an increase in vertical coefficient of

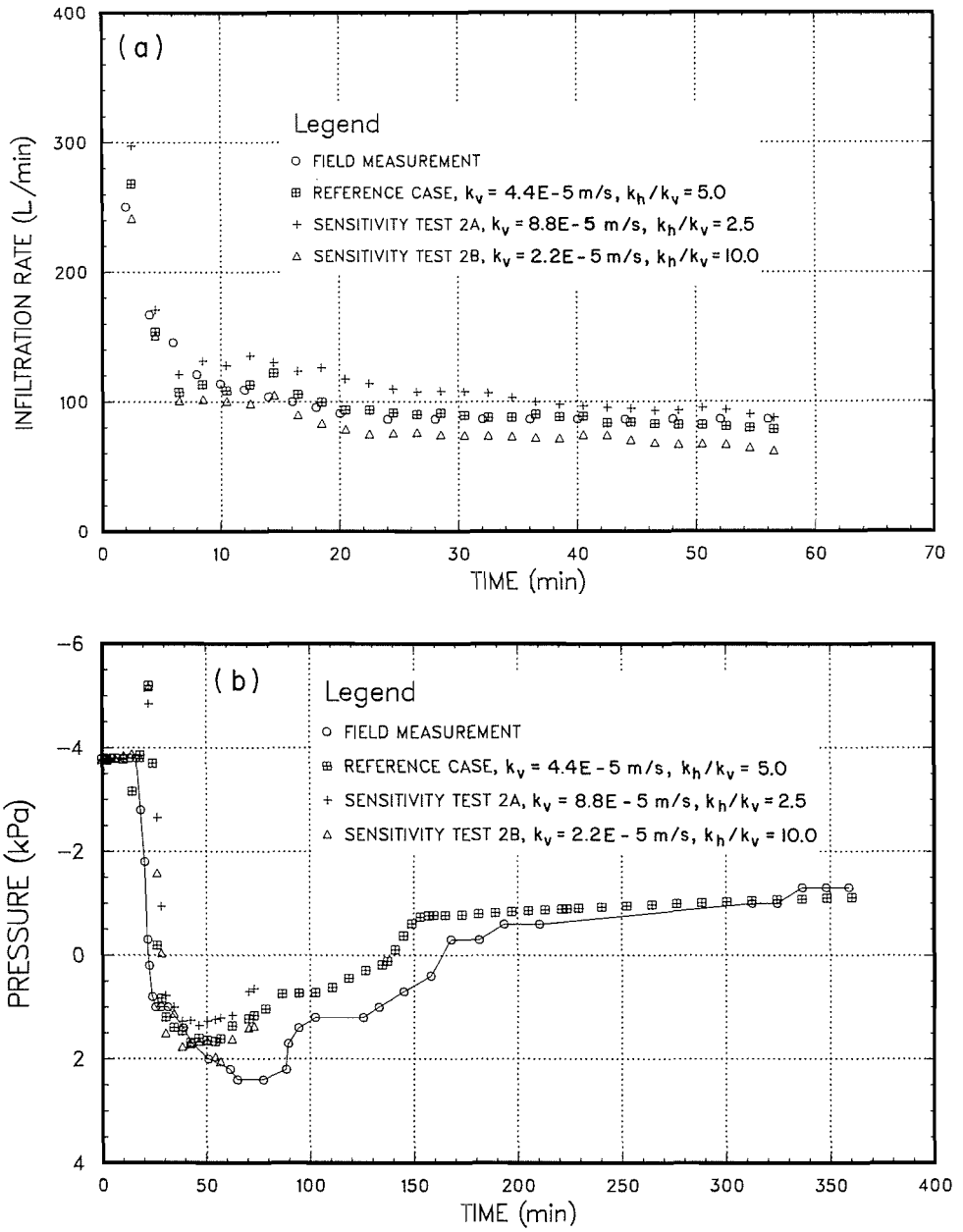

FIG. 14. (*a*) Effect on infiltration rate due to variation of vertical coefficient of permeability; (*b*) effect on pressure response due to variation of vertical coefficient of permeability.

permeability corresponds to a higher infiltration rate and vice versa.

Figures 15*a* and 15*b* demonstrate the effects of the horizontal coefficients of permeability on the simulated infiltration rates and pressure responses. As anticipated, the horizontal coefficient of permeability has a similar effect on the infiltration rate as the vertical coefficient of permeability. However, its influence is even more pronounced, in terms of both initial and final stages of infiltration rates (Fig. 15*a*). The horizontal coefficient of permeability also has a significant influence on the arrival time of the wetting front, as illustrated in Fig. 15*b*. As illustrated in Figs. 13*b* and 15*b*, increasing or decreasing the horizontal permeability would produce similar effects on the arrival time of the wetting front as decreasing or increasing the storage term respectively.

The influence of the degree of anisotropy on the simulated infiltration rate, as well as the pressure response, cannot be interpreted alone and must be considered in conjunction with the vertical and horizontal coefficients of permeability. For example, Fig. 14*a* shows that an increase in the degree of anisotropy can actually result in a decrease in infiltration rate, whereas Fig. 15*a* indicates an increase. Similarly, Fig. 14*b* demonstrates that an increase or a decrease in the degree of anisotropy has no influence on the arrival time of the wetting front, while Fig. 15*b* illustrates that an increase or a decrease in the degree of anisotropy can adversely affect the arrival time of the wetting front.

Conclusions

Simulation of brine infiltration using the described finite element flow model was generally in good agreement with field

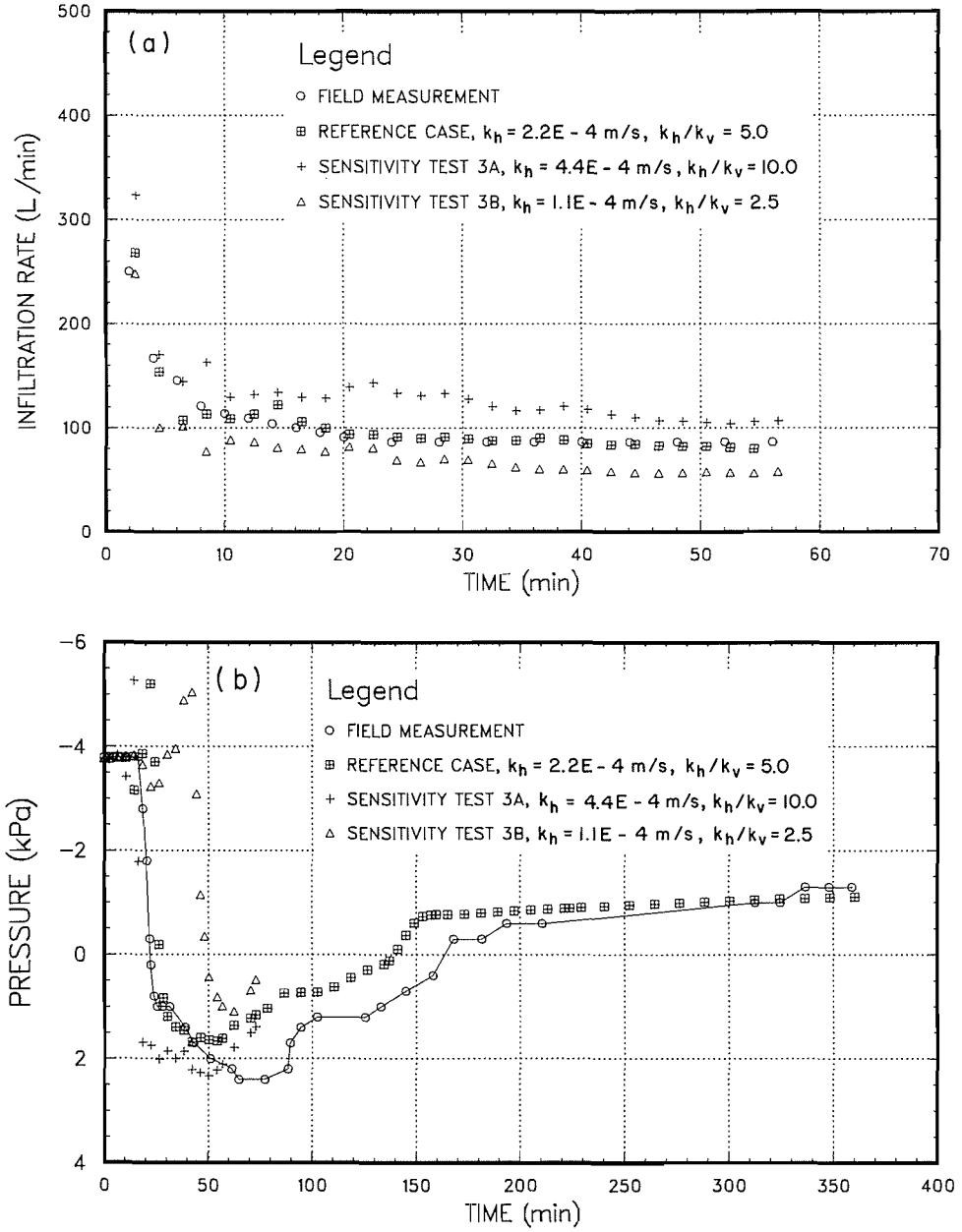

FIG. 15. (*a*) Effect on infiltration rate due to variation of horizontal coefficient of permeability; (*b*) effect on pressure response due to variation of horizontal coefficient of permeability.

measurements. The agreement measured in terms of infiltration rate and pressure response was particularly good considering that no matching of the results was attempted. The implication of the agreement between the field measurements and simulation results is that the saturated and unsaturated flow theory is applicable for modelling the flow of brine through tailings piles. Furthermore, it lends support to the application of the laboratory-determined fluid content versus suction curve, as well as the calculated permeability versus suction curve, to field cases.

The input parameters characterizing the potash tailings were found to have a pronounced influence on the flow of brine through the tailings. In particular, the results of the sensitivity analysis illustrate that the infiltration rate is strongly dependent on the horizontal and vertical coefficients of permeability, and especially the horizontal permeability, which is the major permeability. On the other hand, it is shown that the rate of propagation of the wetting front is predominantly related to the storage term and the degree of anisotropy of the tailings.

The saturated and unsaturated hydraulic properties for the potash tailings and clay slimes have been determined and verified to a certain extent, and these parameters are applicable to those studies pertaining to the flow of brine within the saturated–unsaturated tailings pile. It is, however, noted that "site-specific" or even "location-specific" parameters may be required for carrying out any studies, in view of the variability of the potash tailings and clay slimes observed under field conditions.

Acknowledgement

This study was sponsored by the Potash Corporation of Sas-

katchewan in cooperation with the Department of Civil Engineering, University of Saskatchewan.

CASAGRANDE, A. 1937. Seepage through dams. Journal of the New England Water Works Association, **51**(2): 131–172.

ELZEFTAWY, A., and MANSELL, R. S. 1975. Hydraulic conductivity calculations for unsaturated steady-state flow in sand. Soil Science Society of America Proceedings, **39**: 599–605.

FREDLUND, D. G., and MORGENSTERN, N. R. 1976. Constitutive relations for volume change in unsaturated soils. Canadian Geotechnical Journal, **13**: 261–276.

FREEZE, R. A. 1969. The mechanism of natural groundwater recharge and discharge. 1. One-dimensional vertical, unsteady, unsaturated flow above a recharging or discharging groundwater flow system. Water Resources Research, **5**: 153–171.

———1971. Three-dimensional, transient, saturated–unsaturated flow in a groundwater basin. Water Resources Research, **7**: 347–366.

GREEN, R. E., and COREY, C. 1971. Calculation of hydraulic conductivity: A further evaluation of some predictive methods. Soil Science Society of America Proceedings, **35**: 3–8.

KESSLER, J., and OOSTERBAAN, R. J. 1974. Determining hydraulic conductivity of soils. *In* Drainage principles and applications. Vol. 3. International Institute for Land Reclamation and Improvement, Wageningen, The Netherlands, Publication 16, pp. 253–296.

LAM, L. 1983. Saturated–unsaturated transient finite element seepage model. M.Sc. thesis, University of Saskatchewan, Saskatoon, Sask.

LAM, L., FREDLUND, D. G., and BARBOUR, S. L. 1987. Transient seepage model for saturated–unsaturated soil systems: a geotechnical engineering approach. Canadian Geotechnical Journal, **24**: 565–580.

MCWHORTER, D. G. 1985. Seepage and leakage from dams and impoundments. Proceedings of a symposium sponsored by the Geotechnical Engineering Division in conjuction with the ASCE National Convention, Denver, CO, pp. 200–217.

NEUMAN, S. P. 1973. Saturated–unsaturated seepage by finite elements. ASCE Journal of the Hydraulics Division, **99**(HY12): 2233–2250.

NEUMAN, S. P., and WITHERSPOON, P. A. 1971. Analysis of nonsteady flow with a free surface using the finite element method. Water Resources Research, **7**: 611.

PAPAGIANAKIS, A. T., and FREDLUND, D. G. 1984. A steady state model for flow in saturated–unsaturated soils. Canadian Geotechnical Journal, **21**: 419–430.

PHILIP, J. R. 1957. Numerical solution of equations of the diffusion type with diffusivity concentration-dependent II. Australian Journal of Physics, **10**: 29–42.

REYNOLDS, W. D., ELRICH, D. G., and TOPP, G. C. 1983. A re-examination of the constant head well permeameter method for measuring saturated hydraulic conductivity above water table. Soil Science, **136**: 250–268.

SEGOL, G. 1982. Unsaturated flow modelling as applied to field problems. Proceedings of the Symposium on Unsaturated Flow and Transport Modelling, U.S. Nuclear Regulatory Commission, pp. 35–53.

SMILES, D. C., VACHAUD, G., and VACLIN, M. 1971. A test of the uniqueness of the soil moisture characteristic during transient nonhysteretic flow of water in a rigid soil. Soil Science Society of America Proceedings, **35**: 534–539.

TAYLOR, R. L., and BROWN, C. B. 1967. Darcy flow with a free surface. ASCE Journal of the Hydraulics Division, **93**(HY2): 25–33.

VACHAUD, G., VAUCLIN, M., and WAKIL, M. 1972. A study of the uniqueness of the soil moisture characteristic during desorption by vertical drainage. Soil Science Society of America Proceedings, **36**: 531–532.

WATSON, K. K. 1965. Non-continuous porous media flow. Water Resources Laboratory Report 84, University of New South Wales, Manly Vale, N.S.W., Australia.

WONG, D. K. H. 1985. A study of brine flow through saturated–unsaturated potash tailings. M.Sc. thesis, University of Saskatchewan, Saskatoon, Sask.

WONG. D. K. H., and BARBOUR, S. L. 1985. Studies of the infiltration and migration of brine in salt tailings. Proceedings of the Canadian Society for Civil Engineering Annual Conference, Saskatoon, Sask., Vol. 1A, pp. 357–374.

———1987. Studies of the infiltration and migration of brine in potash tailings. Canadian Journal of Civil Engineering, **14**: 638–648.